*Structural Engineering and Mechanics, Vol. 33, No. 6 (2009) 697-708*
DOI: http://dx.doi.org/10.12989/sem.2009.33.6.697


# Dynamic stress intensity factors for two parallel cracks in an infinite orthotropic plate subject to an impact load

Shouetsu Itou†

*Department of Mechanical Engineering, Kanagawa University, Rokkakubashi, Kanagawa-ku, Yokohama 221-8686, Japan*

*(Received May 12, 2008, Accepted September 25, 2009)*

**Abstract.** Stresses are solved for two parallel cracks in an infinite orthotropic plate during passage of incoming shock stress waves normal to their surfaces. Fourier transformations were used to reduce the boundary conditions with respect to the cracks to two pairs of dual integral equations in the Laplace domain. To solve these equations, the differences in the crack surface displacements were expanded to a series of functions that are zero outside the cracks. The unknown coefficients in the series were solved using the Schmidt method so as to satisfy the conditions inside the cracks. The stress intensity factors were defined in the Laplace domain and were inverted numerically to physical space. Dynamic stress intensity factors were calculated numerically for selected crack configurations.

**Keywords:** orthotropic material; two cracks; dynamic stress intensity factor; composite materials; Fourier transforms; numerical Laplace inversion.

## 1. Introduction

Fiber-reinforced plastics are being used increasingly for machine parts because of their high strength and relatively light weight. Since the matrix is reinforced by fibers, cracks may appear in the matrix along the fibers. Composite materials are essentially orthotropic, and the stresses around the crack can be obtained using the orthotropic theory of elasticity. A static solution for a crack in an infinite orthotropic plate was reported by Ang and Williams (1961), and it was clarified that the stress intensity factors $K_I$ and $K_{II}$ correspond to those for a crack in an infinite isotropic plate. If a crack exists near the stress free boundary, the stress intensity factors may be affected by the material orthotropic property. Based on these considerations, the stresses were solved for two collinear cracks in an orthotropic strip by Delale and Erdogan (1977). In the paper (Delale and Erdogan 1977), the cracks were placed normal to the stress free-boundaries. Later, the stress intensity factors were provided for a crack and for two collinear cracks in an orthotropic strip by Cinar and Erdogan (1983), where the crack was situated parallel to the stress free boundaries of the strip. The composite materials are often weakened by several cracks. To clear the mutual effect of these cracks on the stress intensity factors, the stresses were solved for a main-crack and a parallel micro-crack in an infinite orthotropic plane by Chen and Hasebe (1994). The stress intensity factors were also

† Professor, E-mail: itous001@kanagawa-u.ac.jp

solved for two interacting cracks, one of which coincides with the axis of material orthotropy, with the other being oriented in a general direction (Chen and Hasebe 1995).

If cracked composite materials are loaded dynamically, the stresses are affected by the inertia effect. A time-harmonic solution was first obtained for a crack in an infinite orthotropic plane (Ohyoshi 1973). Later, transient dynamic stress intensity factors were solved for a crack in an infinite orthotropic plane under a load applied suddenly to the crack surfaces (Kassir and Bandyopadhyay 1983). The transient dynamic stress intensity factors were given for the case in which an impact load is applied to the crack surfaces in an orthotropic strip with a central crack situated perpendicular to the stress-free surfaces (Shindo *et al*. 1986). Cracks often initiate from the stress-free surfaces of the strip and travel toward the interior of the strip. Therefore, it is meaningful to solve dynamic edge crack problems. Dynamic stress intensity factors were solved for two symmetrically situated edge cracks in an infinite orthotropic strip under an applied impact load (Shindo *et al.* 1991). The corresponding solutions were also provided for a single edge crack in an orthotropic strip (Shindo *et al.* 1992).

If the functionally graded materials are manufactured by using a plasma spray technique, the material properties may not be isotropic, but orthotropic (Sampath *et al.* 1995, Kaysser and Ilschner 1995). Scattering of anti-plane harmonic waves by a finite crack in the functionally graded orthotropic medium was investigated by Ma *et al.* (2007a). Later, the corresponding problems were also solved for a crack in the functionally graded orthotropic materials under the time-harmonic Mode I and II loadings (Ma *et al.* 2007b).

The dynamic stress intensity factors for two parallel cracks in an infinite isotropic plane were solved for the incident time-harmonic stress waves which impinge normal to the cracks (Takakuda 1982) and it was revealed that the peak values of the dynamic stress intensity factors were considerably larger than those for the corresponding static solution. The corresponding dynamic stresses were solved for two parallel cracks in an infinite isotropic plate during the passage of impact shock stress waves (Itou 1995). In composite materials, cracks have a tendency to appear in the matrix parallel to the fibers. The dynamic stress intensity factors were clarified for two parallel cracks in an infinite orthotropic plane during the passage of the incident time-harmonic stress waves (Itou and Haliding 1997).

The composite materials used in aircraft, vehicles, and other applications are often loaded suddenly. In the present paper, transient dynamic stresses are solved for two parallel cracks in an infinite orthotropic plane during the passage of shock stress waves that propagate normal to the cracks. Using a method similar to that employed in the Refs. (Itou 1995), the boundary conditions were reduced to dual integral equations in the Laplace domain. In order to solve these equations, the differences between the crack surface displacements are expanded to a series of functions that are equal to zero outside the cracks. The Schmidt method explained in Refs. (Morse and Feshbach 1958, Yau 1967, Itou 1976) is then applied to solve the unknown coefficients in the series so as to satisfy the boundary conditions inside the cracks.

If we replace $\omega$ by $(is)$, all the expressions in time-harmonic problems having the time factor $\exp(i\omega t)$ are valid in the Laplace transform in which $\exp(-st)$ is the kernel of the Laplace transformation. Then, it may be considered that solving the transient dynamic problem is trivial because the conversion is quite straightforward. It is true, but the work to convert the problem is not so easy in practice. It is also not easy to make the FORTRAN programming to perform numerical calculations for the dynamic stress intensity factors. Furthermore, it is useful to find the peak values of the dynamic stress intensity factors. In the present paper, it is verified that the incoming shock

stress wave can propagate through the orthotropic medium.

The stress intensity factors defined in the Laplace domain are inverted to physical space using the numerical technique (Miller and Guy 1966). Stress intensity factors are calculated numerically for typical composite materials and for an isotropic material.

## 2. Fundamental equations

Consider a crack located along the $x$-axis from $-a$ to $a$ at $y = 0$, with respect to the rectangular coordinates $(x, y)$, and another along the $x$-axis from $-b$ to $b$ at $y = -h$, as shown in Fig. 1. For convenience, $-h < y < 0$ is referred to as layer (1), $0 < y$ is referred to as upper half-plane (2), and $y < -h$ is referred to as lower half-plane (3). When the problem is solved under the plane stress condition, the equations of motion can be reduced to the following form

$$\begin{aligned} c_{11}\partial^2 u/\partial x^2 + \partial^2 u/\partial y^2 + (1 + c_{12})\partial^2 v/\partial x\partial y &= 1/c_T^2 \times \partial^2 u/\partial t^2 \\ c_{22}\partial^2 v/\partial y^2 + \partial^2 v/\partial x^2 + (1 + c_{12})\partial^2 u/\partial x\partial y &= 1/c_T^2 \times \partial^2 v/\partial t^2 \end{aligned} \tag{1}$$

with

$$c_{11} = E_x/\{\mu_{xy}[1 - (E_y/E_x)\nu_{xy}^2]\}, \quad c_{22} = c_{11}(E_y/E_x), \quad c_{12} = \nu_{xy}c_{22}, \quad c_T = (\mu_{xy}/\rho)^{1/2} \tag{2}$$

where $u$ and $v$ are defined as the $x$ and $y$ components of the displacement, respectively, $E_x$ and $E_y$ are the Young's moduli of the $x$ and $y$ components, respectively, $\mu_{xy}$ is the modulus of rigidity, $\nu_{xy}$ is Poisson's ratio, $\rho$ is the density of the material, and $t$ is time.

The stresses can be expressed as follows

$$\begin{aligned} \sigma_x/\mu_{xy} &= c_{11}\partial u/\partial x + c_{12}\partial v/\partial y, \quad \sigma_y/\mu_{xy} = c_{12}\partial u/\partial x + c_{22}\partial v/\partial y \\ \tau_{xy}/\mu_{xy} &= \partial u/\partial y + \partial v/\partial x \end{aligned} \tag{3}$$

The incident stress wave that propagates along the $y$-axis in the negative direction through the infinite orthotropic plane can be expressed as follows

$$v^{(inc)} = v_0(y + \sqrt{c_{22}}c_T t)H[y + \sqrt{c_{22}}c_T t] \tag{4}$$

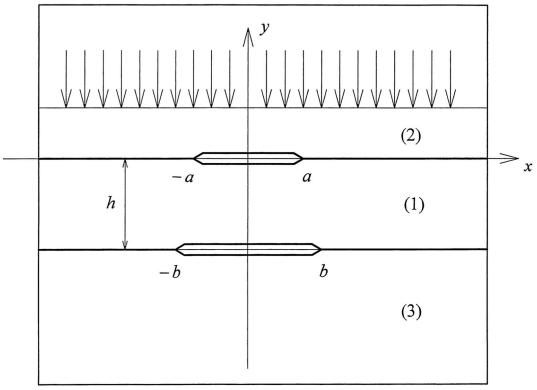


Fig. 1 Geometry and coordinate system

where $v_0$ is a constant and $H(t)$ is the Heaviside unit step function. Time $t$ is considered to be zero when the wave front reaches the upper crack at $y = 0$. Next, Eq. (4) is shown to satisfy the second equation in Eq. (1). Partial differentiating $v^{(inc)}$ with respect to $y$, we obtain

$$\begin{aligned} \partial v^{(inc)}/\partial y &= v_0 H[y+\sqrt{c_{22}}c_T t] + v_0(y+\sqrt{c_{22}}c_T t)\,\delta(y+\sqrt{c_{22}}c_T t) \\ \partial^2 v^{(inc)}/\partial y^2 &= v_0\delta(y+\sqrt{c_{22}}c_T t) + v_0\,\delta(y+\sqrt{c_{22}}c_T t) + v_0(y+\sqrt{c_{22}}c_T t)\delta'(y+\sqrt{c_{22}}c_T t) \end{aligned} \tag{5}$$

$$\begin{aligned} \partial v^{(inc)}/\partial t &= v_0\sqrt{c_{22}}c_T H[y+\sqrt{c_{22}}c_T t] + v_0(y+\sqrt{c_{22}}c_T t)\,\delta(y+\sqrt{c_{22}}c_T t)\sqrt{c_{22}}c_T \\ \partial^2 v^{(inc)}/\partial t^2 &= v_0 c_{22}c_T^2\delta(y+\sqrt{c_{22}}c_T t) + v_0 c_{22}c_T^2\delta(y+\sqrt{c_{22}}c_T t) + v_0(y+\sqrt{c_{22}}c_T t)c_{22}c_T^2\delta'(y+\sqrt{c_{22}}c_T t) \end{aligned} \tag{6}$$

Next, from Eqs. (5) and (6), we obtain the following equations

$$\begin{aligned} c_{22}\partial^2 v/\partial y^2 &= 2c_{22}v_0\,\delta(y+\sqrt{c_{22}}c_T t) + c_{22}v_0(y+\sqrt{c_{22}}c_T t)\delta'(y+\sqrt{c_{22}}c_T t) \\ 1/c_T^2\times\partial^2 v/\partial t^2 &= 2v_0 c_{22}\delta(y+\sqrt{c_{22}}c_T t) + v_0(y+\sqrt{c_{22}}c_T t)c_{22}\delta'(y+\sqrt{c_{22}}c_T t) \end{aligned} \tag{7}$$

Thus, the following equation can be satisfied

$$c_{22}\partial^2 v/\partial y^2 + \partial^2 v/\partial x^2 + (1+c_{12})\partial^2 u/\partial x\partial y\,(=c_{22}\partial^2 v/\partial y^2) = 1/c_T^2\times\partial^2 v/\partial t^2 \tag{8}$$

The expression in Eq. (5) can be converted to the following

$$(y+\sqrt{c_{22}}c_T t)\delta(y+\sqrt{c_{22}}c_T t) = (y+\sqrt{c_{22}}c_T t)\frac{1}{\pi}\int_0^\infty \cos[\xi(y+\sqrt{c_{22}}c_T t)]d\xi \tag{9}$$

Replacing $(y+\sqrt{c_{22}}c_T t)$ in Eq. (9) with $Y$, and letting $Y$ approach zero, we obtain

$$\lim_{Y\to 0}[Y\delta(Y)] = \lim_{Y\to 0}\left\{Y\frac{1}{\pi}\int_0^\infty \cos[\xi Y]d\xi\right\} = \lim_{Y\to 0}\left\{\frac{1}{\pi}\int_0^\infty [Y\cos(\xi Y)]d\xi\right\} = 0 \tag{10}$$

Thus, the first equation in Eq. (5) can be replaced by the following equation

$$\partial v^{(inc)}/\partial y = v_0 H[y+\sqrt{c_{22}}c_T t] \tag{11}$$

As a result, the incident stresses can be expressed by

$$\begin{aligned} \sigma_y^{(inc)} &= pH[y+\sqrt{c_{22}}c_T t] \\ \tau_{xy}^{(inc)} &= 0 \end{aligned} \tag{12}$$

with

$$p = \mu_{xy}c_{22}v_0 \tag{13}$$

Therefore, the boundary conditions for the present problem can be expressed as

$$\sigma_{y2} = \sigma_{y1}, \quad \tau_{xy2} = \tau_{xy1} \qquad \text{at} \quad y = 0, \quad |x| \le \infty \tag{14}$$

$$\sigma_{y1} = \sigma_{y3}, \quad \tau_{xy1} = \tau_{xy3} \qquad \text{at} \quad y = -h, \quad |x| \le \infty \tag{15}$$

$$\sigma_{y2} = -pH(t), \quad \tau_{xy2} = 0 \qquad \text{at} \quad y = 0, \quad |x| \le a \tag{16}$$

$$u_2 = u_1, \quad v_2 = v_1 \qquad \text{at} \quad y = 0, \quad a \le |x| \tag{17}$$

$$\sigma_{y3} = -pH[t - h/(\sqrt{c_{22}}c_T)], \quad \tau_{xy3} = 0 \qquad \text{at} \quad y = -h, \quad |x| \le b \tag{18}$$

$$u_1 = u_3, \quad v_1 = v_3 \qquad \text{at} \quad y = -h, \quad b \le |x| \tag{19}$$

where the subscript 1 indicates the layer, the subscript 2 indicates the upper half-plane (2), and the subscript 3 indicates the lower half-plane (3).

## 3. Analysis

To obtain a solution, the following Laplace transforms are introduced

$$g^*(s) = \int_0^\infty g(t)\exp(-st)dt, \quad g(t) = 1/(2\pi i) \times \int_{Br.} g^*(s)\exp(st)ds \tag{20}$$

and the following Fourier transforms are also introduced

$$\bar{f}(\xi) = \int_{-\infty}^{\infty} f(x)\exp(i\xi x)dx, \quad f(x) = 1/(2\pi i) \times \int_{-\infty}^{\infty} \bar{f}(\xi)\exp(-i\xi x)d\xi \tag{21}$$

Applying Eqs. (20) and (21) to Eq. (1), we obtain

$$\frac{d^4\bar{u}_i^*}{dy^4} + q\frac{d^2\bar{u}_i^*}{dy^2} + r\bar{u}_i^* = 0, \quad \frac{d^4\bar{v}_i^*}{dy^4} + q\frac{d^2\bar{v}_i^*}{dy^2} + r\bar{v}_i^* = 0 \tag{22}$$

with

$$q = -[(c_{11}c_{22} - 2c_{12} - c_{12}^2)/c_{22}]\xi^2 - (1 + c_{22})s^2/(c_{22}c_T^2)$$
$$r = (\xi^2 c_{11} + s^2/c_T^2)(\xi^2 + s^2/c_T^2)/c_{22} \tag{23}$$

The characteristic equation for differential Eq. (22) is given by

$$\lambda^4 + q\lambda^2 + r = 0 \tag{24}$$

Solutions are expressed as follows according to the values of $q$ and $r$

$$\text{for } q^2 - 4r \ge 0 \text{ and } -q + (q^2 - 4r)^{1/2} \ge 0$$
$$\lambda_1 = [-q + (q^2 - 4r)^{1/2}]^{1/2}/\sqrt{2} \tag{25}$$

$$\text{for } q^2 - 4r \ge 0 \text{ and } -q + (q^2 - 4r)^{1/2} < 0$$
$$\lambda_1 = [q - (q^2 - 4r)^{1/2}]^{1/2} i/\sqrt{2} \tag{26}$$

$$\text{for } q^2 - 4r \ge 0 \text{ and } -q - (q^2 - 4r)^{1/2} \ge 0$$
$$\lambda_3 = [-q - (q^2 - 4r)^{1/2}]^{1/2}/\sqrt{2} \tag{27}$$

$$\text{for } q^2-4r\geq 0 \text{ and } -q-(q^2-4r)^{1/2}<0$$
$$\lambda_3=[q+(q^2-4r)^{1/2}]^{1/2}i/\sqrt{2} \tag{28}$$

for $q^2-4r<0$

$$\lambda_1=\sqrt{\eta/2}[\cos(\theta/2)+i\sin(\theta/2)],\quad \lambda_3=\sqrt{\eta/2}[\cos(\theta/2)-i\sin(\theta/2)] \text{ for } \cos(\theta/2)>0$$
$$\lambda_1=-\sqrt{\eta/2}[\cos(\theta/2)+i\sin(\theta/2)],\quad \lambda_3=-\sqrt{\eta/2}[\cos(\theta/2)-i\sin(\theta/2)] \text{ for } \cos(\theta/2)<0 \tag{29}$$

with

$$\eta=2\sqrt{r},\quad \theta=\tan^{-1}[(4r-q^2)^{1/2}/(-q)] \tag{30}$$

For all cases, $\lambda_2$ and $\lambda_4$ are given by

$$\lambda_2=-\lambda_1,\quad \lambda_4=-\lambda_3 \tag{31}$$

For the layer (1), the solutions of Eq. (22) have the following forms

$$\bar{u}_1^*=A_1\cosh(\alpha_1 y)+B_1\cosh(\beta_1 y)+C_1\sinh(\alpha_1 y)+D_1\sinh(\beta_1 y)$$
$$\bar{v}_1^*=E_1\cosh(\alpha_1 y)+F_1\cosh(\beta_1 y)+G_1\sinh(\alpha_1 y)+H_1\sinh(\beta_1 y) \tag{32}$$

with

$$\alpha_1=\lambda_1,\quad \beta_1=\lambda_3 \tag{33}$$

where $A_1, B_1, \ldots, H_1$ are unknown coefficients. For the upper half-plane (2) and the lower half-plane (3), the solutions of Eq. (22) have the following forms in terms of the unknown coefficients $A_2, B_2, \ldots, D_3$

$$\bar{u}_2^*=A_2\exp(\alpha_2 y)+B_2\exp(\beta_2 y),\quad \bar{v}_2^*=C_2\exp(\alpha_2 y)+D_2\exp(\beta_2 y)$$
$$\bar{u}_3^*=A_3\exp(\alpha_3 y)+B_3\exp(\beta_3 y),\quad \bar{v}_3^*=C_3\exp(\alpha_3 y)+D_3\exp(\beta_3 y) \tag{34}$$

The real parts of $\alpha_2$ and $\beta_2$ must be negative, whereas those of $\alpha_3$ and $\beta_3$ must be positive. The real parts of $\alpha_2$, $\beta_2$, $\alpha_3$, and $\beta_3$ are given as

$$\alpha_2=\lambda_2,\quad \beta_2=\lambda_4,\quad \alpha_3=\lambda_1,\quad \beta_3=\lambda_3 \tag{35}$$

Substituting Eqs. (32) and (34) into Eq. (22), we obtain

$$A_1=iG_1\times(1+c_{12})\alpha_1\xi/m_1,\quad B_1=iH_1\times(1+c_{12})\beta_1\xi/n_1$$
$$C_1=iE_1\times(1+c_{12})\alpha_1\xi/m_1,\quad D_1=iF_1\times(1+c_{12})\beta_1\xi/n_1$$
$$A_2=iC_2\times(1+c_{12})\alpha_2\xi/m_2,\quad B_2=iD_2\times(1+c_{12})\beta_2\xi/n_2$$
$$A_3=iC_3\times(1+c_{12})\alpha_3\xi/m_3,\quad B_3=iD_3\times(1+c_{12})\beta_3\xi/n_3 \tag{36}$$

with

$$m_i=(1+c_{12})\alpha_i\xi/(\alpha_i^2-s^2/c_T^2-c_{11}\xi^2)$$
$$n_i=(1+c_{12})\beta_i\xi/(\beta_i^2-s^2/c_T^2-c_{11}\xi^2)\qquad \text{for } (i=1,2,3) \tag{37}$$

Hereinafter, the mathematical derivation is basically the same as that of a previous paper (Itou and Haliding 1997). If $\omega$ is replaced by $(is)$ in the previous paper (Itou and Haliding 1997), all of the expressions are valid in the present paper. Therefore, the previous paper is described only briefly. The stresses and displacements can be expressed by eight unknowns: $G_1$, $H_1$, $E_1$, $F_1$, $C_2$, $D_2$, $C_3$, and $D_3$. Using Eqs. (14) and (15), which are valid for $|x| \le \infty$, the eight unknowns are reduced to four unknowns $C_2, D_2, C_3, D_3$.

The differences of the displacements are expanded in the Laplace domain as follows

$$\begin{aligned} \pi(u^*_{1a} - u^*_{2a}) &= \sum_{n=1}^{\infty} a_n \sin[2n \times \sin^{-1}(x/a)] \qquad \text{for} \quad |x| \le a \\ &= 0 \qquad\qquad\qquad\qquad\qquad\qquad\quad \text{for} \quad a \le |x| \end{aligned} \tag{38}$$

$$\begin{aligned} \pi(v^*_{1a} - v^*_{2a}) &= \sum_{n=1}^{\infty} b_n \cos[(2n-1)\sin^{-1}(x/a)] \qquad \text{for} \quad |x| \le a \\ &= 0 \qquad\qquad\qquad\qquad\qquad\qquad\quad \text{for} \quad a \le |x| \end{aligned} \tag{39}$$

$$\begin{aligned} \pi(u^*_{1b} - u^*_{3b}) &= \sum_{n=1}^{\infty} c_n \sin[2n \times \sin^{-1}(x/a)] \qquad \text{for} \quad |x| \le b \\ &= 0 \qquad\qquad\qquad\qquad\qquad\qquad\quad \text{for} \quad b \le |x| \end{aligned} \tag{40}$$

$$\begin{aligned} \pi(v^*_{1b} - v^*_{3b}) &= \sum_{n=1}^{\infty} d_n \cos[(2n-1)\sin^{-1}(x/a)] \qquad \text{for} \quad |x| \le b \\ &= 0 \qquad\qquad\qquad\qquad\qquad\qquad\quad \text{for} \quad b \le |x| \end{aligned} \tag{41}$$

where $a_n, b_n, c_n$, and $d_n$ are unknowns, and the subscripts $a$ and $b$ indicate the values at $y = 0$ and $y = -h$, respectively. If the differences of the displacements are expanded by Eqs. (38)-(41), then boundary conditions (17) and (19) have been satisfied. Then, the remaining boundary conditions (16) and (18), which must be satisfied inside the cracks, reduce to the forms

$$\begin{aligned} &\sum_{n=1}^{\infty} a_n k_{na}(x) + \sum_{n=1}^{\infty} b_n l_{na}(x) + \sum_{n=1}^{\infty} c_n m_{na}(x) + \sum_{n=1}^{\infty} d_n n_{na}(x) = -u(x) \\ &\sum_{n=1}^{\infty} a_n o_{na}(x) + \sum_{n=1}^{\infty} b_n p_{na}(x) + \sum_{n=1}^{\infty} c_n q_{na}(x) + \sum_{n=1}^{\infty} d_n r_{na}(x) = 0 \qquad \text{for} \quad |x| \le a \end{aligned} \tag{42}$$

$$\begin{aligned} &\sum_{n=1}^{\infty} a_n k_{nb}(x) + \sum_{n=1}^{\infty} b_n l_{nb}(x) + \sum_{n=1}^{\infty} c_n m_{nb}(x) + \sum_{n=1}^{\infty} d_n n_{nb}(x) = -v(x) \\ &\sum_{n=1}^{\infty} a_n o_{nb}(x) + \sum_{n=1}^{\infty} b_n p_{nb}(x) + \sum_{n=1}^{\infty} c_n q_{nb}(x) + \sum_{n=1}^{\infty} d_n r_{nb}(x) = 0 \qquad \text{for} \quad |x| \le b \end{aligned} \tag{43}$$

where known functions $k_{na}(x), l_{na}(x), \ldots, r_{nb}(x)$ have the same expressions provided by Eq. (C3) in Appendix C in the previous paper (Itou and Haliding 1997), and $u(x)$ and $v(x)$ are given by

$$u(x) = p/s, \qquad v(x) = p\exp[-hs/(\sqrt{c_{22}}c_T)]/s \tag{44}$$

The unknowns $a_n, b_n, c_n$, and $d_n$ in Eqs. (42) and (43) can now be solved using the Schmidt method (Morse and Feshbach 1958, Yau 1967, Itou 1976).

## 4. Stress intensity factors

Once the unknown coefficients $a_n, b_n, c_n$, and $d_n$ have been solved, all of the stresses and displacements can be obtained. The stress intensity factors in the Laplace domain can be expressed as

$$\begin{aligned} K^*_{\mathrm{I}a} &= \lim_{x\to a+}\sqrt{2\pi(x-a)}\,\sigma^*_{y2a} \\ &= \sum_{n=1}^{\infty} b_n\times(2n-1)\times(-1)^n Q^L_2/(\pi a)^{1/2} \\ K^*_{\mathrm{II}a} &= \lim_{x\to a+}\sqrt{2\pi(x-a)}\,\tau^*_{xy2a} \\ &= \sum_{n=1}^{\infty} a_n\times 2n\times(-1)^n Q^L_5/(\pi a)^{1/2} \end{aligned} \tag{45}$$

$$\begin{aligned} K^*_{\mathrm{I}b} &= \lim_{x\to b+}\sqrt{2\pi(x-b)}\,\sigma^*_{y3b} \\ &= \sum_{n=1}^{\infty} d_n\times(2n-1)\times(-1)^n Q^L_{12}/(\pi b)^{1/2} \\ K^*_{\mathrm{II}b} &= \lim_{x\to b+}\sqrt{2\pi(x-b)}\,\tau^*_{xy4b} \\ &= \sum_{n=1}^{\infty} c_n\times 2n\times(-1)^n Q^L_{15}/(\pi b)^{1/2} \end{aligned} \tag{46}$$

where the known constants $Q^L_i(i=2,5,12,15)$ have the same expressions given in Eq. (41) in the previous paper (Itou and Haliding 1997).

The inverse Laplace transformations of the stress intensity factors are carried out by the numerical method described in Ref. (Miller and Guy 1966). When the Laplace transform $g^*(s)$ can be evaluated at discrete points given by

$$s=(\beta+1+k),\quad k=0,1,2,\ldots \tag{47}$$

the coefficients $C_M$ are determined using

$$\delta\times g^*[(k+\beta+1)\delta]=\sum_{M=0}^{k} C_M k!/[(k+\beta+1)(k+\beta+2)\ldots(k+\beta+1+M)(k-M)!] \tag{48}$$

where, $\delta\geq 0$ and $\beta\geq -1$. If the coefficients are calculated up to $C_{N-1}$, an approximate value of $g(t)$ can be found, as follows

$$g(t)=\sum_{M=0}^{N-1} C_M P_M^{(0,\beta)}[2\exp(\delta t)-1] \tag{49}$$

where $P_M^{(\alpha,\beta)}(z)$ is a Jacobi polynomial. The parameters $\delta$, $\beta$, and $N$ must be selected such that $g(t)$ can best be described within a particular range of time $t$.

The relation between $g^*(s)$ and $g(t)$ is then obtained as

$$\lim_{s \to 0}[sg(s)] = \lim_{t \to \infty} g(t) \tag{50}$$

Therefore, the static results of the stress intensity factors in physical space can be obtained using Eq. (50).

## 5. Numerical examples

The dynamic stress intensity factors were calculated numerically with quadruplex precision using a Fortran program. Here, overflow and underflow do not occur within the range $10^{-5500}$ to $10^{+5500}$. Numerical calculations are carried out for graphite-epoxy composites and for steel. The material properties for the composites are provided in a handbook (Peters 1998), and these are given in Table 1, in which the material properties for steel are also presented. For steel, Eq. (24) has two kinds of multiple roots because $E_x$ is equal to $E_y$. In this case, solutions given by Eqs. (32) and (34) are invalid. However, if $E_y$ is replaced by $E_y \times 0.999$, the expressions given by Eqs. (32) and (34) are still valid. In Table 1, the density of the material $\rho$ is not shown, because a dimensionless time $c_T t/a [= (\mu_{xy}/\rho)^{1/2} \times t/a]$ is used instead of time $t$.

The semi-infinite integrals, which appear in the known functions $k_{na}(x), l_{na}(x), \ldots, r_{nb}(x)$, must be evaluated numerically. It can be verified that the numerical integrations have been performed satisfactorily because the integrands decay rapidly as the integration variable $\xi$ increases. To solve

Table 1 Material properties

| Constants | Materials Steel | Graphite-Epoxy Composites |
|---|---|---|
| $E_x$ (GPa) | 206.0 | 145.0 |
| $E_t$ (GPa) | 206.0×0.999 | 9.6 |
| $\mu_{xy}$ (GPa) | 82.4 | 5.8 |
| $\nu_{xy}$ | 0.25 | 0.30 |

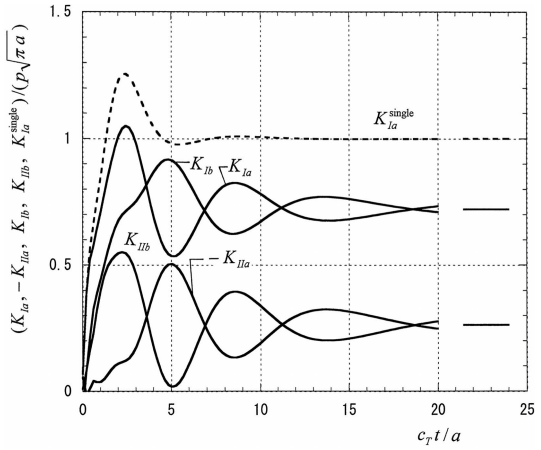


Fig. 2 Stress intensity factors $K_{Ia}$, $K_{IIa}$, $K_{Ib}$, and $K_{IIb}$ for graphite-epoxy composites ($b/a = 1.0$ and $h/a = 0.2$)

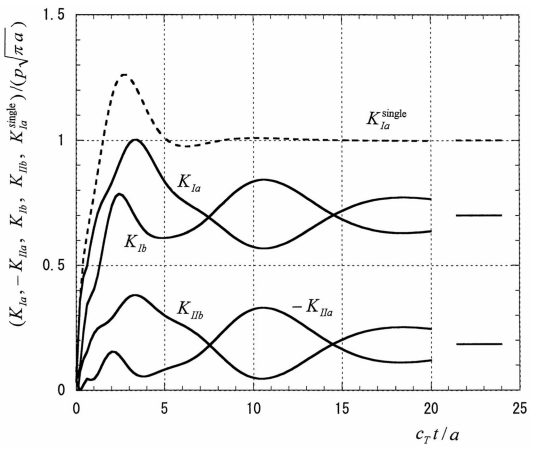


Fig. 3 Stress intensity factors $K_{Ia}$, $K_{IIa}$, $K_{Ib}$, and $K_{IIb}$ for steel ($b/a = 1.0$ and $h/a = 0.2$)

the unknown coefficients $a_n, b_n, c_n$, and $d_n$, the Schmidt method has been applied by truncating the infinite series in Eqs. (42) and (43) by summing from $n = 1$ to $n = 10$. It has been verified that the values for the left-hand side of Eqs. (42) and (43) coincide to those for the right-hand side with acceptable accuracy. The numerical Laplace inversions are carried out by setting ($\beta = 0.0, \delta = 0.2, N = 11$) in Eq. (49).

The stress intensity factors $K_{Ia}, K_{IIa}, K_{Ib}$, and $K_{IIb}$ are calculated for $b/a = 1.0$ and $h/a = 0.2$ and these are plotted with respect to $c_T t/a$ for graphite-epoxy composites and for steel in Figs. 2 and 3, respectively. The corresponding values $K_{Ia}^{\text{single}}$ for a single crack in an infinite plane are solved separately, and these are shown by the dotted lines in these figures. The straight lines drawn on the right-hand side show the corresponding static values calculated using Eq. (50).

## 6. Conclusions

Based on the numerical calculations outlined above, the following conclusions are obtained:

(1) For composite materials weakened by two parallel cracks, the significant stress intensity factor is $K_{Ia}/(p\sqrt{\pi a})$ at the end of the upper crack. The peak value, $K_{Ia}^{peak}/(p\sqrt{\pi a})$ for $b/a = 1.0$ and $h/a = 0.2$, is approximately 1.05 for graphite-epoxy composites and is considerably smaller than 1.25, which is the corresponding value for a single crack in an infinite orthotropic plate. For an isotropic material, the peak value, $K_{Ia}^{peak}/(p\sqrt{\pi a})$ for $b/a = 1.0$ and $h/a = 0.2$, is considerably smaller than that for a single crack in an infinite plate.

(2) The value of $K_{Ia}$ reaches the first peak value, and somewhat later, that of $K_{Ib}$ reaches the peak value. However, for Mode II, the peak value first appears in $K_{IIb}$, and somewhat later, $(-K_{IIa})$ reaches its first peak value.

(3) For a single crack in an infinite plane, the dynamic stress intensity factor increases continuously, eventually reaching the upper peak value. The dynamic stress intensity factor then tends to fall, eventually reaching the lower peak value. Somewhat later, the value converges at the corresponding static value. In contrast, the dynamic stress intensity factors around the two parallel cracks oscillate toward the corresponding static values.

## 7. Correction

The elastic constant $c_{11}$ is given by Eq. (2) as follows

$$c_{11} = E_x/\{\mu_{xy}[1-(E_y/E_x)\nu_{xy}^2]\} \tag{51}$$

In the previous paper (Itou and Haliding 1997), the authors mistakenly presented the following expression

$$c_{11} = E_x\{1-(E_y/E_x)\nu_{xy}^2\}/\mu_{xy} \tag{52}$$

If $\mu_{xy}$ in Eq. (52) is replaced by the following

$$\mu_{xy} \to \{1-(E_y/E_x)\nu_{xy}^2\}^2\mu_{xy} \tag{53}$$

then all of the expressions in the previous paper by (Itou and Haliding 1997) are applicable. In the

paper (Itou and Haliding 1997), the absolute values of the dynamic stress intensity factors are plotted with respect to the dimensionless circular frequency $\omega a/c_T$, which is given by the following equation

$$\omega a/c_T = \omega a/\sqrt{\mu_{xy}/\rho} \tag{54}$$

The modulus of rigidity $\mu_{xy}$ does not appear in the numerical calculations in the previous paper (Itou and Haliding 1997), but their numerical results are the correct values.

Using the correct Eq. (51), the dynamic stress intensity factors have been recalculated numerically, and numerical results are verified to correspond to those provided of the previous paper (Itou and Haliding 1997).

## References


Ang, D.D. and Williams, M.L. (1961), "Combined stresses in an orthotropic plate having a finite crack", *J. Appl. Mech.,* ASME, **28**, 372-378.

Chen, Y.H. and Hasebe, N. (1994), "Interaction between a main-crack and a parallel micro-crack in an orthotropic plane elastic solid", *Int. J. Solids Struct.*, **31**, 1877-1890.

Chen, Y.H. and Hasebe, N. (1995), "Interaction of two off-axis cracks exhibiting orthotropic and general anisotropic behavior under arbitrary extension", *Theor. Appl. Fract. Mec.*, **22**, 249-260.

Cinar, A. and Erdogan, F. (1983), "The crack and wedging problem for an orthotropic strip", *Int. J. Fract.*, **23**, 83-102.

Delale, F. and Erdogan, F. (1977), "The problem of internal and edge cracks in an orthotropic strip", *J. Appl. Mech.,* ASME, **44**, 237-242.

Itou, S. (1976), "Axisymmetric slipless indentation of an infinite elastic hollow cylinder", *Bull. Cal. Math. Soc.*, **68**, 157-165.

Itou, S. (1995), "Dynamic stress intensity factors around two parallel cracks in an infinite elastic plate", *Acta Mech.*, **108**, 87-99.

Itou, S. and Haliding, H. (1997), "Dynamic stress intensity factors around two parallel cracks in an infinite-orthotropic plane subjected to incident harmonic stress waves", *Int. J. Solids Struct.*, **34**, 1145-1165.

Kassir, M.K. and Bandyopadhyay, K.K. (1983), "Impact response of a cracked orthotropic medium", *J. Appl. Mech.,* ASME, **50**, 630-636.

Kaysser, W.A. and Ilschner, B. (1995), "FGM research activities in Europe", *MRS Bull.*, **20**, 22-26.

Ma, L., Li, J., Abdelmoula R. and Wu, L.Z. (2007a), "Dynamic stress intensity factor for cracked functionally graded orthotropic medium under time-harmonic loading", *Eur. J. Mech. A*, **26**, 325-336.

Ma, L., Nie, W., Wu, L.Z. and Guo, L.C. (2007b), "Scattering of anti-plane stress waves by a crack in a non-homogeneous orthotropic medium", *Comp. Struct.*, **79**, 174-179.

Miller, M. and Guy, W.T. (1966), "Numerical inversion of the Laplace transform by use of Jacobi polynomials", *SIAM J. Numer. Anal.*, **3**, 624-635.

Morse, P.M. and Feshbach, H. (1958), *Methods of Theoretical Physics*, Vol. 1, McGraw-Hill, New York.

Ohyoshi, T. (1973), "Effect of orthotropy on singular stresses for a finite crack", *J. Appl. Mech.,* ASME, **40**, 491-497.

Peters, S.T. (Editor) (1998), *Handbook of Composites*, Chapman & Hall, London.

Sampath, S., Herman, H., Shimoda, N. and Saito, T. (1995), "Thermal spray processing of FGMs", *MRS Bull.*, **20**, 27-31.

Shindo, Y., Nozaki, H. and Higaki, H. (1986), "Impact response of a finite crack in an orthotropic strip", *Acta Mech.*, **62**, 87-104.

Shindo, Y., Higaki, H. and Nozaki, H. (1991), "Impact response of symmetric edge cracks in an orthotropic strip", *JSME Int. J., Series I*, **34**, 7-12.

Shindo, Y., Higaki, H. and Nozaki, H. (1992), "Impact response of a single edge crack in an orthotropic strip", *J.*

*Appl. Mech.,* ASME, **59**, S152-S157.
Takakuda, K. (1982), "Scattering of plane harmonic waves by cracks", *Trans. Jap. Soc. Mech. Eng., Series A*, **48**, 1014-1020.
Yau, W.F. (1967), "Axisymmetric slipless indentation of an infinite elastic cylinder", *SIAM J. Appl. Math*., **15**, 219-227.